Available online at www.sciencedirect.com
ScienceDirect
Journal of Photochemistry and Photobiology A: Chemistry 189 (2007) 23–29
Journal of Photochemistry and Photobiology A:Chemistry
www.elsevier.com/locate/jphotochem

Photophysical and photochemical behavior of nimodipine and felodipine

Nancy Pizarro [a,*], Germán Günther [b], Luis J. Núñez-Vergara [a]

[a] *Laboratorio de Bioelectroquímica, Departamento de Química Farmacológica y Toxicológica, Facultad de Ciencias Químicas y Farmacéuticas, Universidad de Chile, P.O. Box 233, Santiago, Chile*

[b] *Laboratorio de Cinética y Fotoquímica, Departamento de Química Orgánica y Fisicoquímica, Facultad de Ciencias Químicas y Farmacéuticas, Universidad de Chile, P.O. Box 233, Santiago, Chile*

Received 30 June 2006; received in revised form 5 January 2007; accepted 8 January 2007
Available online 12 January 2007

Abstract

A different photophysical and photochemical behavior has been found between two second generation antihypertensive 1,4-dihydropyiridines (1,4-DHPs), felodipine and nimodipine. While nimodipine was observed as being more reactive and photolabile in excited state, felodipine showed a major reactivity in its ground state towards an electrophilic transient species like singlet oxygen. Nimodipine had a photodegradation quantum yield of 2.34×10^{-4} in deaereated acetonitrile and 1.81×10^{-2} in deaereated ethanol. The values of the photodegradation quantum yields in aereated solutions were similar. However, felodipine is less photolabile than nimodipine, with a photodegradation quantum yield changing from 1.4×10^{-5} to 7×10^{-6} in the same solvents, probably a consequence of a lowered stability of the zwitterion radical involved in the formation of the photoproduct. In addition, nimodipine and felodipine were able to generate singlet oxygen with quantum yields of 0.085 and 0.003 in benzene, respectively. The results show that tested 1,4-DHPs behave as relatively good scavengers of excited oxygen, with overall rate constant values for nimodipine ranging from $0.38 \times 10^5\ M^{-1}\ s^{-1}$ in chloroform to $9.73 \times 10^5\ M^{-1}\ s^{-1}$ in *N*,*N*-dimethylformamide. On the other hand, the rate constants for felodipine ranged from $0.44 \times 10^5\ M^{-1}\ s^{-1}$ in benzene to $19.5 \times 10^5\ M^{-1}\ s^{-1}$ in *N*,*N*-dimethylacetamide. In conclusion, the present results indicate that it is difficult to discriminate which specie is responsible for the photoallergic and phototoxic effects previously reported for these drugs, because these effects could be attributed to the participation of zwitterionic radicals in the process of photodegradation and/or its ability to generate singlet oxygen.

Keywords: 1,4-Dihydropyridines; Photophysical behavior; Photochemistry; Singlet oxygen; Mechanisms

1. Introduction

Felodipine and nimodipine are calcium channel blockers of the second-generation of 1,4-dihydropyridines (1,4-DHPs), which are widely used as antihypertensive drugs [1,2]. They block the entrance of extracellular calcium into vascular and cardiac muscles with different selectivity, resulting in a reduction of blood pressure associated with its vasodilatory action [3,4]. In addition, they also have other biological activities, such as the ability of scavenge reactive oxygen species (ROS) [5,6].

These calcium channel blockers have been associated with adverse photosensitive effects at skin level [7,8]. However, very few studies related to their photochemical behavior have been published. In order to understand the mechanisms involved in their phototoxic activities, it is necessary to identify the reactive excited states involved, the transient species, and the photoproduct generated [9]. Furthermore, it is important to determine the capacity of these drugs to generate reactive oxygen species, such as singlet oxygen [10]. Singlet oxygen, $O_2(^1\Delta_g)$, can react with biological substrates as well as with the same drug, yielding other photoactive species or toxic products and reduce the drug pharmacological effect. Usually, the self-sensitized drug photooxidation (or singlet oxygen physical quenching) is barely considered, although it would be important because if $O_2(^1\Delta_g)$ is quenched, it will not be available to react with other biologically relevant substrates or produce pharmacological effects. The aim of this study is to contribute to the knowledge of the photochemical and photophysical processes involved in the photodegradation of two well-known and widely used second-generation 1,4-DHPs, named nimodipine and felodipine (Fig. 1).

* Corresponding author. Tel.: +56 2 9782865; fax: +56 2 9782868.
E-mail address: npizarro@ciq.uchile.cl (N. Pizarro).

1010-6030/$ – see front matter © 2007 Elsevier B.V. All rights reserved.
doi:10.1016/j.jphotochem.2007.01.003

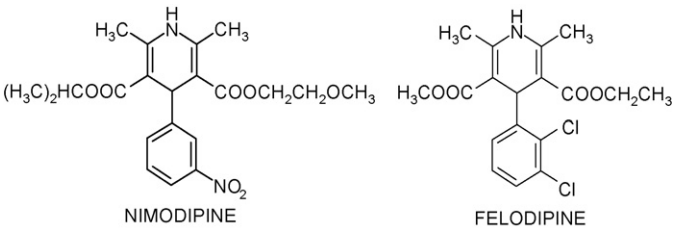

Fig. 1. Chemical structures of nimodipine and felodipine.

2. Experimental

2.1. Drugs and reagents

Nimodipine (1,4-dihydro-2,6-dimethyl-4-(3-nitrophenyl)-3,5-pyridinedicarboxylic acid 2-methoxyethyl 1-methylethyl ester) and felodipine (4-(2,3-dichlorophenyl)-1,4-dihydro-2,6-dimethylpyridine-3,5-pyridinedicarboxylic acid ethyl methyl ester) (Sigma) were used as received. 5,10,15,20-Tetraphenyl-21H,23H-porphine (TPP), 9,10-dimethylanthracene (DMA), phenalenone and 1,3-diphenylisobenzofurane (DPBF) (Aldrich) were used without further purification. Rose Bengal (RB) (Fluka) was recrystallized from ethanol prior to use. All solvents (Merck) were of spectroscopic or HPLC grade. *cis*-1,3-Pentadiene (*cis*-piperylene) (Fluka) was distilled prior to use.

2.2. Apparatus and procedures

UV–vis absorption spectra and steady state competitive kinetic experiments were performed in a Unicam UV-4 spectrophotometer. A GC/MS system (Hewlett-Packard Gas Chromatograph model 5890 series II equipped with Fisons Mass Selective Detector MD800 and a Hewlett-Packard Ultra-2 capillary column (25 m)), was used to obtain electron impact mass spectra. Fluorescence experiments were carried out in a Fluorolog Tau-2 spectrofluorimeter (SPEX, Jobin Ybon).

Photolysis experiments were done with 1×10^{-4} M solutions (3 mL) of the 1,4-DHPs in several selected solvents which were purged with Argon for 20 min in a 10 mm fluorescence quartz cell sealed with a septum. The solutions were irradiated with a Black Ray UV lamp with a 366 nm filter. The radiant flux was determined as described in literature [11].

Chemical reaction rate constants were determined in several selected solvents using a light-protected by black paint 10 mL double-wall cell. A centered window allowed irradiation with light of a given wavelength by using appropriate cut-off filters. Circulating water maintained the cell temperature at 22 ± 0.5 °C. Sensitizer irradiation (RB or TPP) was performed with a visible, 200 W, Par lamp. A Hewlett-Packard Gas Chromatograph model 5890 series II equipped with a NPD detector and a Hewlett-Packard Ultra-2 capillary column was used to monitor substrate consumption. FID detector was used to follow the *cis*-piperylene consumption and conversion to the *trans*-isomer. DMA and DPBF were the actinometers.

Time-resolved luminescence measurements were carried out in 1 cm pathlength fluorescence cells. The sensitizer (TPP or RB) was excited by the second harmonic (532 nm, nominal power ca. 9 mJ/pulse) of a 6 ns light pulse of a Quantel Brilliant Q-Switched Nd:YAG laser. A liquid-nitrogen cooled North Coast germanium photodiode detector with a built-in preamplifier was used to detect infrared radiation from the cell. The detector was at right-angle to the cell. An interference filter (1270 nm, Spectrogon US, Inc.) and a cut-off filter (995 nm, Andover Corp.) were the only elements between the cell face and the diode cover plate. Preamplifier output was fed into the 1 MΩ input of a digitizing oscilloscope. Computerized experiment control, data acquisition and analysis were performed with LabView based software developed at the Laboratory of Kinetics and Photochemistry of the University of Chile.

Laser flash photolysis was performed with a Q-switched Nd:YAG laser (532 nm, ca. 9 mJ/pulse). The monitoring light beam – a 150 W Xe lamp mounted in a PTI lamp housing system – was passed through a water filter before impinging on the entrance of the cell holder. An electronic shutter – between the water filter and the cell holder controlled by a shutter driver/timer – was triggered by the Q-switch from the laser. Two lenses and slits were used to collimate and focus the monitoring light to the cell holder and to the entrance slit of the monochromator. A Hamamatsu R-928 photomultiplier detector mounted in a homemade housing was fitted to the monochromator exit slit port. PMT signals were monitored with a Hewlett-Packard 54540A 500 MHz, 1Gsa digital oscilloscope used in DC mode. An external PTI optical beam divider was employed to trigger the oscilloscope. The signals can be stored and averaged in the same scope at the repetition rate of the laser pulse (10 Hz) or can be fed to a personal computer equipped with home-designed software for data acquisition and treatment. The incident beam was perpendicular to the surface of the sample and the output signal was observed in right angle with the normal.

Singlet oxygen quantum yields (ϕ_Δ) were measured in time-resolved phosphorescence experiments using phenalenone as the actinometer ($\phi_\Delta = 0.98$ in acetonitrile, $\phi_\Delta = 0.93$ in benzene and $\phi_\Delta = 0.97$ in ethanol) [12], by comparing the response of the detector extrapolated to zero time and zero laser power, the latter adjusted with a set of neutral density filters. Optically matched solutions of drug and actinometer in the same solvent, were excited by the third harmonic (355 nm, ca. 28 mJ/pulse) of the Nd:YAG laser.

Equation coefficients and statistical parameters of LSER correlations were obtained by multilinear correlation analysis with STAT VIEW 5.0 (SAS Institute Inc.). Results agreed with the *t*-statistic of descriptors.

3. Results and discussion

3.1. Photophysics and photochemistry of 1,4-dihydropyridines

Nimodipine and felodipine exhibit the typical UV–vis absorption spectra of 4-phenyl-1,4-dihydropiridines derivatives; two characteristic absortion bands at 230 and 350 nm due to the presence of dihydropyridine chromofore (Fig. 2). When solutions of these compounds are irradiated with UV light, the

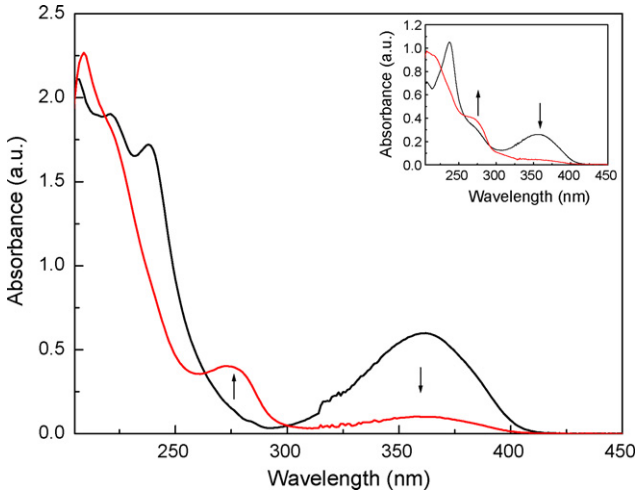

Fig. 2. Time–course absorption spectra upon UV light irradiation of nimodipine solutions. Inset shows time–course absorption spectra upon UV light irradiation of felodipine solutions.

absortion band centered at 350 nm decreases with the appearance of a new UV absorption at 280 nm. The main photodegradation product for both 1,4-DHPs was the corresponding pyridine derivative, which is the chromofore responsible for the new band at 280 nm. These drugs have a very poor emission (fluorescence) implying that deactivation through radiative processes is not favored. Fasani et al. [13] proposed that the lowest singlet excited state of these compounds is deactivated by a fast intramolecular electron transfer from the dihydropyridine ring to the substituted phenyl ring, yielding a zwitterionic radical as the intermediary species. This proposition is compatible with the minor fluorescense emission detected for nimodipine than the emission for felodipine, because the presence of the nitro moiety in comparison with the chloro group in the 4-phenyl substituent, would help to delocalizate the charge of the zwitterionic species, and then, the intramolecular electron transfer is more favored in a nitrophenyl substituted 1,4-DHP. In addition, we were not able to detect triplet excited states or transient species in our flash photolysis experiments, which is in agreement with the proposed deactivation process.

The first order photodegradation rate constants for nimodipine and felodipine were determinated by following the 1,4-DHPs consumption through GC technique (Table 1). Consumption quantum yields were measured using the 9,10-dimethylanthracene self-sensitized photooxygenation as actinometer [11]. The data in Table 1 clearly demostrate a different behavior for nimodipine and felodipine. The highest values of photodegradation kinetic constant of nimodipine are nearly independent of the presence of oxygen; whereas the lowest values of photodecomposition kinetic constant of felodipine increase in aerated solutions. The evaluated kinetic values for nimodipine were similar to the reported by Fasani et al. [13]. Also, we tried to identificate the excited state which would be responsible for the photoproduct formation, using a triplet quencher like *cis*-piperylene. This compound undergoes photosensitized *cis–trans*-isomerization in the presence of triplet excited state [14], and it has also been involved in the deactivation of singlet excited states without *cis–trans*-isomerization [15,16], so the conversion to the *trans*-isomer would be indicative of a triplet excited state participation. The fluorescence intensity of nimodipine, but not felodipine, was quenched by the addition of a different concentration of *cis*-piperylene. The bimolecular rate constant for the quenching of the singlet excited state of nimodipine in benzene was calculated using a Stern–Volmer fit with a value of ca. 10^9 M^{-1} s^{-1}.

Fig. 3 shows first order kinetic plot for the photodegradation of nimodipine in benzene. When the photodegradation is carried out in the presence of *cis*-piperylene, the rate of the process decreases significantly. Gas chromatography experiments showed that the formation of the main photoproduct was also inhibited. However, a low conversion of the *cis*-piperylene in its *trans*-isomers was observed. Similar results were found for felodipine; the presence of *cis*-piperylene inhibits the rate of the photodegradation proccess and the photoproduct formation. In this case, *cis*-piperylene does not undergo any isomerization. This could mean that in both cases, the main degradation pathway occurs through the lowest singlet excited state, with a minimal contribution in the case of the nimodipine from its triplet excited state. The zwitterionic biradical intermediate generated by the fast intramolecular electron transfer lead to the principal photoproduct – the pyridine derivative – by a intermolecular proton transfer to the solvent. This would explain the existence of higher kinetic constants in methanol as compared to other solvents.

Table 1
First order kinetic constants, k, and quantum yields, ϕ, of photodegradation of 1,4-dihydropryridines

Solvent	Nimodipine		Felodipine	
	k (10^{-5} min^{-1})	ϕ (10^{-5} molec/abs. phot.)	k (10^{-5} min^{-1})	ϕ (10^{-5} molec/abs phot.)
Acetonitrile				
Purged	99.2	23.4	8.5	1.4
Aerated	75.6	20.0	3.44	8.3
Benzene				
Purged	6750	770	7.4	1.1
Aerated	7000	630	50.1	7.4
Ethanol				
Purged	9380	1810	4.2	0.7
Aerated	9910	1130	89.4	14.5

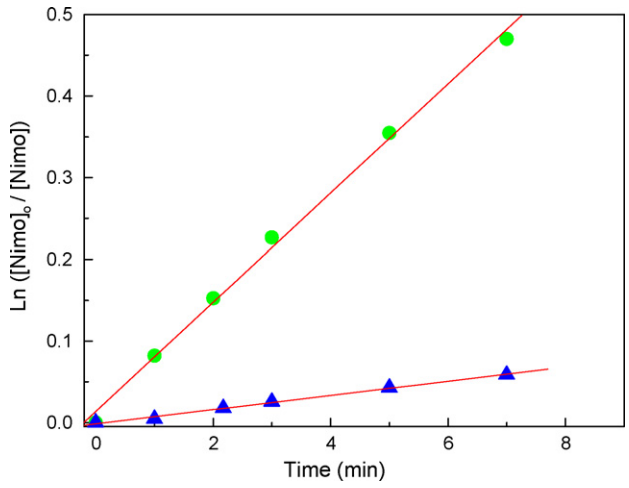

Fig. 3. First order plot for the photodegradation of nimodipine in benzene: (●) in the abscence and (▲) in the presence of *cis*-piperylene.

3.2. Generation of singlet oxygen by 1,4-DHP derivatives

Measurements of singlet oxygen generation quantum yield (ϕ_Δ) were carried out by using the phosphorescence method [17], following the intensity of $O_2(^1\Delta_g)$ luminescence decay at 1270 nm, after the excitation of either nimodipine or felodipine with pulses of the third harmonic of a Nd–YAG laser at 355 nm (Fig. 4). The values obtained in benzene were 0.085 and 0.003 for nimodipine and felodipine, respectively, using phenalenone as the actinometer. Singlet oxygen generation was only detected in a non-polar medium, and no phosphorescence emission was observed in more polar solvents, such as acetonitrile and ethanol. Despite the fact that the ϕ_Δ values are small, they could be significant at biological level since this 1,4-DHP derivatives can accumulate in membranes due to its high lipophilicity [2,18], where the singlet oxygen generation would be more efficient.

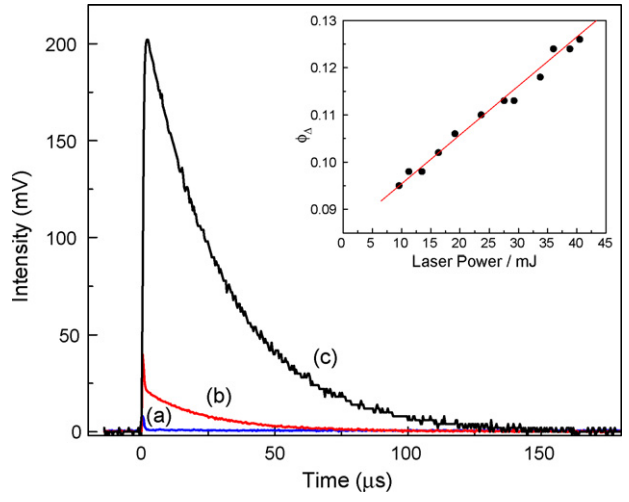

Fig. 4. Luminescence decay of $O_2(^1\Delta_g)$ at 1270 nm, generated after the excitation. At 355 nm of (a) felodipine, (b) nimodipine and (c) phenalenone with third harmonic pulses of Nd–YAG laser in benzene. The inset shows the quantum yields of the photosensitized generation of $O_2(^1\Delta_g)$ by nimodipine in benzene, as a function of the laser power of the excitation source.

Singlet oxygen generation from nimodipine, may be explained considering the proposition of Fasani et al. for deactivation of nitro-substituted 1,4-DPHs [13]. The lowest singlet excited state is deactivated by a fast intramolecular electron transfer from the dihydropyridine ring to the substituted phenyl ring to give a zwitterionic biradical intermediate, which would yield photoproducts or through a back-electron transfer would give an excited triplet state. The lower ϕ_Δ observed for felodipine is compatible with the above proposition because the presence of chloro atoms in the phenyl ring diminish the possibility of stabilization of the zwitterionic biradical intermediate, when compared with the presence of a nitro group in such aromatic ring. Therefore, it is less probable that the back-electron transfer does produce the triplet state.

3.3. Reactivity of 1,4-DHP derivatives towards singlet oxygen

Using time-resolved phosphorescence detection (TRPD), the total (physical and chemical) quenching rate constants, k_T, for the reaction of $O_2(^1\Delta_g)$ with nimodipine and felodipine in several solvents were determined. Singlet oxygen lifetimes were evaluated in the absence (τ_0^{-1}) and in the presence (τ^{-1}) of different concentrations of the 1,4-dihydropyridines. Total rate constant, k_T, was obtained according to the Stern–Volmer treatment Eq. (1).

$$\tau^{-1} = \tau_0^{-1} + k_T\,[1,4\text{-DHP}] \quad (1)$$

Linear plots of τ^{-1} versus 1,4-DHP concentration were obtained in all the employed solvents. The intercept of these plots matches closely with previously reported singlet oxygen lifetime in the same solvents [19]. The deactivation of sensitizer excited states (singlet or triplet) by 1,4-DHPs was not observed under our experimental conditions.

The k_T values obtained in different solvents are summarized in Table 2. The reactivity of both 1,4-DHPs towards singlet oxygen is similar, with total quenching rate constants in the same order, being the overall rate constants solvent-dependent. For nimodipine, k_T increases around 10-fold for solvent changes from benzene to methylacetamide, whereas the k_T for felodipine shows 44-fold increase.

The chemical quenching rate constants, k_R, for the 1,4-DHPs were determined in several selected solvents employing TPP as the sensitizer, and monitoring the drug consumption with gas chromatography. DMA and DPBF were used as actinometers to determine the $O_2(^1\Delta_g)$ steady-state concentration. The values of k_R obtained from the slope of the pseudo first order plots are shown in Table 2. From the data, it can be concluded that felodipine shows a higher chemical reactivity than nimodipine. Also, the rate constants (k_T or k_R) for both 1,4-DHPs have the same dependence on solvent polarity. In addition, both the chemical and the overall rate constants were similar for felodipine, indicating that the main pathway of singlet oxygen deactivation is the reactive channel yielding photooxidation product. In contrast, for nimodipine, k_R values are lower than k_T values, although in the most polar solvents the chemical reaction is also the main deactivation path of $O_2(^1\Delta_g)$.

Table 2
Total quenching (k_T) and chemical (k_R) rate constant for reactions of 1,4-DHP derivatives with singlet oxygen

Solvent	Nimodipine		Felodipine	
	k_T (10^5 M^{-1} s^{-1})	k_R (10^5 M^{-1} s^{-1})	k_T (10^5 M^{-1} s^{-1})	k_R (10^5 M^{-1} s^{-1})
Methanol	1.10	–	3.03	–
Ethanol	1.23	–	2.74	2.09
n-Propanol	1.66	–	1.32	–
Acetonitrile	3.36	0.91	8.62	3.41
Acetone	2.05	–	2.50	–
Ethyl acetate	0.85	–	1.62	–
Dioxane	2.71	–	6.19	–
Benzene	0.89	0.11	0.44	0.47
Methylene chloride	1.76	–	1.28	–
Chloroform	0.38	–	1.33	–
N,*N*-Dimethylformamide	9.73	6.46	18.1	21.0
N,*N*-Dimethylacetamide	8.52	–	19.5	–
Propylencarbonate	6.67	5.27	17.1	17.8

k_T and k_R errors are within 10% for all results.

The dye-sensitized photooxygenation of both studied 1,4-DHPs yields the corresponding 2,3-dichlorophenyl and 3-nitrophenyl pyridine derivatives as the main product. The isolated products were characterized and identified by GC–MS technique.

In order to obtain additional information about the microscopic nature of the interaction involved in the first step of the reaction between 1,4-DHPs and $O_2(^1\Delta_g)$, the rate constant dependence on solvent microscopic parameters was analyzed [20] by using the semiempirical solvatochromic equation (LSER) of Reichardt [21] and Kamlet et al. [22]:

$$\log k = \log k_0 + a\alpha + b\beta + s\pi^* + d\delta + h\rho_H^2 \quad (2)$$

where α is the hydrogen bond donation ability of the solvent (HBD), β the hydrogen bond acceptance (HBA) or electron-pair donation ability to form a coordinative bond and π^* is the polarity/polarizability parameter. The parameter δ is a correction term for polarizability, which takes a value of 1.0 for aromatic solvents, 0.5 for polyhalogenated aliphatic solvents, and 0 for all other aliphatic solvents. The Hildebrand's solubility parameter, ρ_H, corresponds to the square root of the solvent cohesive density, being a measure of the disruption of solvent–solvent interactions in creating a solute cavity. The solvent-independent coefficients *a*, *b*, *s*, *d* and *h* are characteristic of the process and indicative of the rate constant sensitivity to each solvent property, accounting for the established specific interactions at microscopic level between solute and solvent during the formation/stabilization of the encounter complex (exciplex in some cases).

The coefficients of the LSER equation obtained by multilinear correlation analysis for the dependence of k_T on solvent parameters are given in Table 3. These values result from purely statistical criteria. The overall quality of equation is indicated by sample size, *N*; correlation coefficient, *R*; standard deviation, S.D.; and Fisher index of equation reliability, *F*. The reliability of each term is indicated by a large *t*-statistics, *t*-stat; two-tail probability, *P*(two-tail) < 0.05; and the VIF statigraph (a measure of parameter orthogonally) is near to 1. Good quality is indicated by large *N* and *F* values, small S.D. and *R* close to 1. Results show that not all the descriptors are significant. Descriptor coefficients accepted in the correlation equation were those with a significance level ≥0.95. For this reason, α and β parameters were not included in the LSER correlation. According to the coefficients of the equations shown in Table 3, the k_T values for both 1,4-DHPs increase in solvents with the largest capacities to stabilize charges and dipoles, and increase in solvents with high cohesive energy.

In a previous study was found a similar dependence of k_T on solvent parameters for the interaction of singlet oxygen with nifedipine and nitrendipine [23]. These findings were explained in terms of the formation of an encounter complex with charge separation due to the attack of singlet oxygen on the carbon–carbon double bond of the dihydropyridine ring yielding a perepoxide-like exciplex [24–26]. The rate constant dependence on the π^* parameter accounts for the charge separation in the exciplex, and the dependence on Hildebrand's parameter, ρ_H, indicates liberation of solvent molecules as consequence of the exciplex formation. According to the present results, the same mechanism accounts for the interaction of singlet oxygen with nimodipine and felodipine, so the reactive center is one of the dihydropyridine double bond. The major reactivity of felodipine towards singlet oxygen could be understood in terms of the minor inductive electron withdrawing effect of the 2,3-dichlorophenyl substituent in comparison with the 3-nitrophenyl group. Only

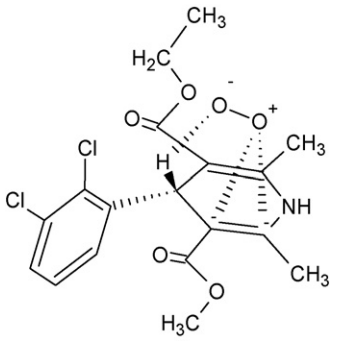

Fig. 5. Proposed encounter complex formed in the first step of the reaction of singlet oxygen with felodipine.

Table 3
LSER correlation equations for the reaction of singlet oxygen with nimodipine, felodipine and nifedipine

Nimodipine	$\log k_0$	s	d	h
Coefficient	3.403	2.663	–	0.001
±	0.278	0.344		0.001
t-Stat	12.257	7.751		0.948
P(two-tail)	<0.0001	0.0001		0.3748
VIF		1.008		1.008
	$R = 0.949$, S.D. = 0.147, $F = 31.400$, $N = 10$			
Felodipine	$\log k_0$	s	d	h
Coefficient	3.252	3.025	−0.606	0.002
±	0.300	0.336	0.169	0.001
t-Stat	10.826	8.977	−3.590	1.960
P(two-tail)	<0.0001	0.0001	0.0115	0.0976
VIF		1.008		1.008
	$R = 0.979$, S.D. = 0.140, $F = 45.387$, $N = 10$			
Nifedipine [23]	$\log k_0$	s	d	h
Coefficient	6.278	0.317	−0.277	0.002
±	0.208	0.213	0.113	0.001
t-Stat	30.224	1.486	−2.446	2.473
P(two-tail)	<0.0001	0.1755	0.0402	0.0385
VIF		1.316		1.316
	$R = 0.901$, S.D. = 0.097, $F = 11.523$, $N = 12$			

$\log k = \log k_0 + s\pi^* + d\delta + h\rho_H^2$.

inductive electron effect should be operative between the dihydropyridinic and substituted-phenyl moieties. This is due to the fact that both the sp^3 hybridization of carbon atom in position 4 and the lack of coplanarity between phenyl and the dihydropyridine ring (forming 62° dihedral angle [13]). The structure proposed for the exciplex is illustrated in Fig. 5.

The perepoxide-like exciplex can be stabilized by an intramolecular interaction involving the allylic hydrogen and the negatively charged terminal oxygen of perepoxide [24]. Also, an electron withdrawing and sterically demanding substituent like the ester substituent produces a "geminal effect", which promotes the abstraction of the allylic hydrogen on C-4 [25,27]. The hydroperoxide intermediate formed upon hydrogen abstraction evolves to the main product, the pyridine derivative. For an *ortho*-nitroaryl substituted 1,4-DHP (nifedipine), the interaction between the labile hydrogen at C-4 and the *ortho*-nitro group has been reported [28,29], which increases the charge density on the dihydropirydine ring. This electronic effect allows to explain the larger reactivity of nifedipine towards singlet oxygen compared with other substituted 1,4-DHPs [23].

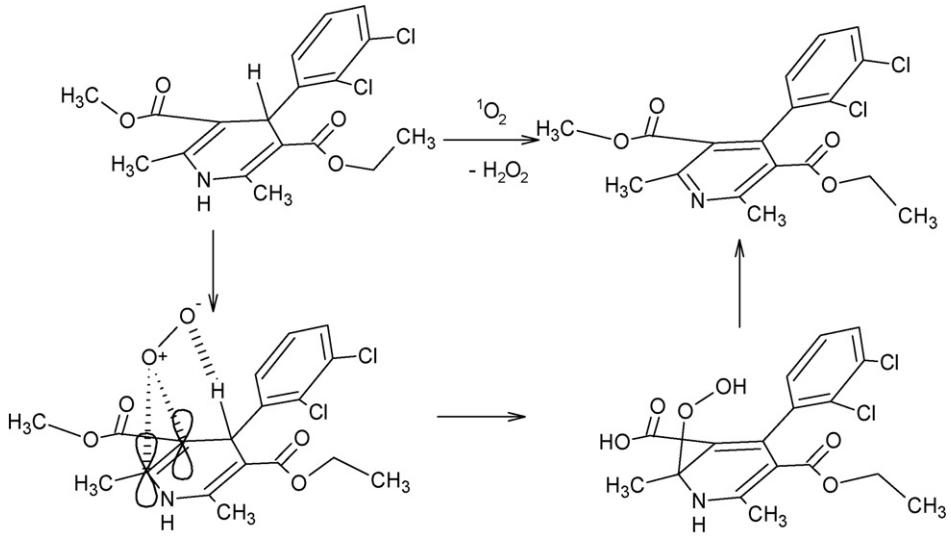

Fig. 6. Proposed mechanism for the reaction of $O_2(^1\Delta_g)$ with felodipine.

Nevertheless, such interaction would be also responsible of the lower nifedipine k_R values, because it would prevent the stabilization of negatively charged oxygen of perepoxide with the allylic hydrogen. Due to the major electron density over the reactive center of nifedipine (the carbon–carbon double bond in the dihydropyridine ring), the electrophilic attack of singlet oxygen, could have a more concerted character, producing an encounter complex with less charge separation. In the case of nimodipine and felodipine, the perepoxide-like exciplex should have a larger charge separation, because the coefficients associated with the π^* parameters are greater than that reported for nifedipine (Table 3). The larger charge separation can be explained due to both effects; the absence of the intramolecular interaction between the aryl-substituent and the hydrogen at C-4 and the inductive electron withdrawing effect of 2,3-dichlorophenyl and 3-nitrophenyl substituents. The more compact structure of the exciplex, may account for the k_T dependence on ρ_H^2 parameter, since its formation involves release of solvent molecules.

The highest k_R values are for the chemical reaction between singlet oxygen and felodipine. This result could be explained in terms of more labile hydrogen bonded to nitrogen at the 1-position in the dihydropyrdine ring, which could assist the rearrangement of the hydroperoxide intermediate to yield the pyridine derivative (Fig. 6).

4. Conclusions

The results show that nimodipine and felodipine have different photophysical and photochemical behaviors due to the presence of substituents on the 4-phenyl moiety. The 3-nitrophenyl group favors intramolecular electron transfer yielding a zwitterionic biradical intermediate, which can evolve to dihydropyridine localized triplet or to pyridine derivative as main photodegradation product. The presence of 2,3-dichlorophenyl group diminishes the efficiency of the intramolecular electron transfer, explaining the lower values of the kinetic parameters obtained for felodipine.

The tendency of nimodipine to generate $O_2(^1\Delta_g)$ with major efficiency than felodipine would be consistent with the more efficient formation of zwitterionic biradical intermediate.

On the other hand, the presence of 2,3-dichlorophenyl group in comparison with the 3-nitrophenyl group, increases the reactivity of felodipine towards singlet oxygen. This drug behaves as a good scavenger of the excited oxygen. The interaction of felodipine with singlet oxygen is mainly via the reactive pathway yielding the pyridine derivative as photooxidation product.

The dependence of the overall rate constants of the deactivation of singlet oxygen by the 1,4-DHPs on solvent properties permits us to sustain the proposal of the perepoxide-like encounter complex formation with a partial separation of charge. This complex leads to a hydroperoxide and then yields the nitropyridine derivative as the main photooxidation product.

The present results indicate that photoallergic and phototoxic effects observed for these drugs could be attributed to the participation of the zwitterionic biradical in the process of photodegradation and/or to its ability for the generation of singlet oxygen.

Acknowledgements

This work was financially supported by FONDECYT, Grant No. 3030048. Thanks are also given to Dr. Antonio Zanocco for useful discussions and for the use of the facilities of the Laboratory of Kinetics and Photochemistry of the Faculty of Chemistry and Pharmaceutical Science of University of Chile.

Appendix A. Supplementary data

Supplementary data associated with this article can be found, in the online version, at doi:10.1016/j.jphotochem.2007.01.003.

References

[1] D.J. Trigglen, Drug Dev. Res. 58 (2003) 5–17.
[2] P.A. Van Zwieten, Blood Pressure 7 (1998) 5–9.
[3] B. Ljung, J. Cardiovasc. Pharmacol. 15 (1990) 11–16.
[4] Y. Ono, K. Mizuno, M. Goto, S. Hashimoto, T. Watanabe, Curr. Ther. Res. 60 (1999) 392–401.
[5] L. Cominacini, A.F. Pasini, U. Garbin, A.M. Pastorino, A. Davoli, C. Nava, M. Campagnola, P. Rossato, V. Lo Cascioa, Biochem. Biophys. Res. Commun. 302 (2003) 679–684.
[6] G. Supinski, D. Nethery, D. Stofan, A. DiMarco, J. Appl. Physiol. 87 (1999) 2177–2185.
[7] S.M. Cooper, F. Wojnarowska, Clin. Exp. Dermatol. 28 (2003) 588–591.
[8] J.F. Silvestre, M.P. Albares, L. Carnero, R. Botella, J. Am. Acad. Dermatol. 45 (2001) 323–324.
[9] G. Cosa, J.C. Scaiano, Photochem. Photobiol. 80 (2004) 159–174.
[10] C. Schweitzer, R. Schmidt, Chem. Rev. 103 (2003) 1685–1757.
[11] H.J. Kuhn, S.E. Braslavsky, R. Schmidt, Pure Appl. Chem. 76 (2004) 2105–2146.
[12] C. Schmidt, R. Tanielian, C. Dunsbach, J. Wolff, Photochem. Photobiol. A 79 (1994) 11–17.
[13] E. Fasani, M. Fagnoni, D. Dondi, A. Albini, J. Org. Chem. 71 (2006) 2037–2045.
[14] G.S. Hammond, N.J. Turro, P.A. Leermakers, J. Phys. Chem. 66 (1962) 1144–1147.
[15] T.R. Evans, P.A. Leermakers, J. Am. Chem. Soc. 91 (1969) 5898–5900.
[16] B.M. Vittimberga, D.F. Sears, J. Heterocyclic. Chem. 37 (2000) 291–295.
[17] J.C. Scaiano, R.W. Redmond, B. Mehta, J.T. Arnanson, Photochem. Photobiol. 52 (1990) 655–659.
[18] I. Mak, P. Boheme, W. Wegliki, Circ. Res. 70 (1992) 1099–1103.
[19] F. Wilkinson, J. Phys. Chem. Ref. Data 24 (1995) 663–1021.
[20] E. Lemp, A.L. Zanocco, E.A. Lissi, Curr. Org. Chem. 7 (2003) 799–819.
[21] C. Reichardt, Solvents and Solvent Effects in Organic Chemistry, second ed., VCH, Weinheim, 1990.
[22] M.J. Kamlet, J.L. Abboud, M.H. Abraham, R.W. Taft, J. Org. Chem. 48 (1983) 2877–2887.
[23] N.A. Pizarro-Urzúa, L.J. Núñez-Vergara, J. Photochem. Photobiol. A 175 (2005) 129–137.
[24] M. Stratakis, M. Orfanopoulos, Tetrahedron 56 (2000) 1595–1615.
[25] E. Clennan, Tetrahedron 56 (2000) 9151–9179.
[26] Y. Yoshioka, S. Yamada, T. Kawakami, M. Nishino, K. Yamaguchi, I. Saito, Bull. Chem. Soc. Jpn. 69 (1996) 2683–2699.
[27] M. Orfanopoulos, C.S. Foote, Tetrahedron Lett. 26 (1985) 5991–5994.
[28] A. Buttafava, A. Faucitano, E. Fasani, A. Albini, A. Ricci, Res. Chem. Intermed. 28 (2002) 231–237.
[29] E. Fasani, D. Dondi, A. Ricci, A. Albini, Photochem. Photobiol. 82 (2006) 225–230.